A FAMILY OF QUASI-VARIABLE MESHES HIGH-RESOLUTION COMPACT OPERATOR SCHEME FOR BURGER'S-HUXLEY AND BURGER'S-FISHER EQUATION

NAVNIT JHA AND MADHAV WAGLEY

Abstract. We describe a quasi-variable meshes implicit compact finite-difference discretization having an accuracy of order four in the spatial direction and second-order in the temporal direction for obtaining numerical solution values of generalized Burger's-Huxley and Burger's-Fisher equations. The new difference scheme is derived for a general one-dimension nonlinear parabolic partial differential equation on a quasi-variable meshes network. The magnitude of local truncation error of the high-order compact scheme remains unchanged in the case of a uniform mesh. Quasi-variable meshes high-order compact formulation yield a more precise solution than uniform meshes high-order schemes of the same magnitude. A detailed exposition of the new scheme has been introduced and discussed the Fourier stability theory. The computational results with generalized Burger's-Huxley equation and Burger's-Fisher equation are obtained using a quasi-variable meshes high-order compact scheme. It is compared with a numerical solution using uniform meshes high-order schemes to demonstrate capability and accuracy.

1. Introduction

The quasi-linear parabolic partial differential equations (PPDEs) play an important role in engineering and physical sciences such as convection effect, diffusion transport interaction, option pricing, fluid flow, and image processing. We list some of the famous examples to one-dimension PPDEs in the literature. Generalized Burger's-Huxley equation (GBHE) was used to describe the interaction between convection, diffusion, and advection. The GBHE model has applications in propagating signals in the nervous system, elasticity, gas dynamics, and heat conduction. The GBHE mathematical model takes the form,

$$\epsilon W^{xx} = W^t + \alpha W^\rho W^x + \beta W(W^\rho - 1)(W^\rho - \sigma), 0 < x < 1, t > 0, \tag{1.1}$$

The associated initial and boundary values are

$$W(x,0) = \left[\frac{\sigma}{2} + \frac{\sigma}{2}\tanh(ax)\right]^{1/\rho}, \tag{1.2}$$

$$W(0,t) = \left[\frac{\sigma}{2} + \frac{\sigma}{2}\tanh(-abt)\right]^{1/\rho}, W(1,t) = \left[\frac{\sigma}{2} + \frac{\sigma}{2}\tanh(a(1-bt))\right]^{1/\rho}, \tag{1.3}$$

and equation (1.1) at $\epsilon = 1$, possesses an analytic solution

$$W(x,t) = \left[\frac{\sigma}{2} + \frac{\sigma}{2}\tanh(a(x-bt))\right]^{1/\rho}, \tag{1.4}$$

where
$$a = \frac{-\alpha\rho + \rho\sqrt{\alpha^2 + 4\beta(1+\rho)}}{4(1+\rho)}, \; b = \frac{\alpha\sigma}{1+\rho} + \frac{(1+\rho-\sigma)(\alpha + \sqrt{\alpha^2 + 4\beta(1+\rho)})}{2(1+\rho)}.$$

The term W^{xx} represents dissipation, α as advection coefficient to the nonlinear advection term $W^\rho W^x$ and $\beta \geq 0, \rho > 0, 0 < \sigma < 1$. For $\alpha = \rho = 1, \beta = 0$, it is Burgers equation that combines nonlinear wave motion with linear diffusion and is a simple model for analyzing the joint effect of diffusion and nonlinear advection. The small positive parameter $\epsilon = R_e^{-1}$, where R_e is Reynold's number. When $\alpha = 0, \beta = \epsilon = 1$, equation (1.1) reduces to Huxley equation [18, 19, 20, 38]. For $\alpha = -1, \beta = \rho = \epsilon = 1$, the equation (1.1) represents Burgers-Huxley equation [6]. The Zeldovich equation appearing in combustion theory is the special case of equation (1.1) when $\alpha = 0$ and $\rho = \epsilon = 1$ are substituted in this equation [10]. When $\alpha = 0, \beta = \rho = \epsilon = 1$, it is FitzHug-Nagumo equation, and it arises in neurobiology for the study of nerve impulses, and it describes the electrical event occurring during impulse transmission along an axon. The FitzHug-Nagumo equation has also gained considerable attention for studying wave propagation in several areas such as, in flame propagation, circuit theory, biology, population genetics and Brownian motion process [27].

Generalized Burgers-Fisher equation (GBFE) is an important model that appears in plasma physics, turbulence, traffic flow, and gas dynamics. GBFE has convective phenomenon from Burgers equation, diffusion transport and reaction behavior from Fisher equation [11]. The GBFE mathematical model is given by
$$\epsilon W^{xx} = W^t + \alpha W^\rho W^x + \beta W(W^p - 1), 0 < x < 1, t > 0. \tag{1.5}$$
The choice $\alpha = 0, \rho = \epsilon = 1$ in the equation (1.5) yields Fishers equation that is used to describe the expansion of biological populations [2, 32]. For $\alpha = 0, \rho = 2, \epsilon = 1$, it describes Rayleigh-Benard convection [7, 42]. The mathematical model
$$\epsilon W^{xx} = W^t - \alpha W + \beta W^\rho, \tag{1.6}$$

where $0 < \epsilon << 1, \alpha, \beta$ are real parameters, and ρ is an integer represents Newell-Whitehead-Segel equation, and it has applications in ecology, mechanical engineering, biology, bio-engineering, stripe pattern, Faraday instability, and Rayleigh-Benard convection. It models the interaction of diffusion with a non-linear effect of the reaction. The term W^t in the equation (1.6) expresses the variations with time at a fixed location, W^{xx} expresses the variations with the spatial variable at a specified time, and $\alpha W - \beta W^\rho$ is the source term [11]. By changing β to $-\beta$ in the equation (1.6), it is Kolmogorov-Petrovskii Piskunov equations, and it arises in the study of tumor growth, an evolution of a dominant gene, transmission of nerve impulses, combustion waves, and heat mass transfer [10, 21].

The mathematical models (1.1)-(1.6) can be broadly expressed as a quasi-linear form in the following manner:
$$\epsilon W^{xx} = \psi(x, t, W, W^x, W^t), (x, t) \in \Omega = (0, 1) \times (0, \infty), \tag{1.7}$$
along with the initial condition
$$W(x, 0) = \phi(x), 0 \leq x \leq 1, \tag{1.8}$$
and the Dirichlets boundary data
$$W(0, t) = F_1(t), W(1, t) = F_2(t), t \geq 0. \tag{1.9}$$
We suppose that ϕ, F_1, F_2 are continuous and the function $\psi \in C^2(\Omega)$, so that their necessary high-order derivatives exist for the application of finite Taylors series expansion. The quasi-linear PPDEs (1.7) along with given values (1.8) and (1.9) are used to determine the unknown function $W = W(x, t)$, which depends on spatial variable x and temporal variable t, inside the domain $\Omega \times [0, \infty), \Omega = [0, 1]$.

For the arbitrary choice of the function ψ, the exact or closed form of a solution may not be possible. Therefore, it is customary to analyze them numerically via some approximating mechanism. There are various approaches for constructing an approximate solution to PPDEs. Numerical treatments to such type of problems by exponential approximations, compact scheme, and high-order methods have been discussed in the past [4, 8, 13, 29, 37, 39, 40, 46]. Sinc-Galerkin and collocation method for solving linear singularly perturbed one-dimension convection-diffusion equations have been developed in [23, 24, 25]. Mohanty and Sharma [36] described a two-level implicit off-step spline in compression discretization of order three in space and two in time or the system PPDEs. Uniform meshes second-order accurate Crank-Nicolson type scheme has gained popularity for solving (1.7) and such a lower order convergent method was described by Jacques [17]. A three-point compact discretization on non-uniform meshes for boundary value problems appeared in electrochemical kinetic simulations has obtained by Bieniasz [26]. A stable, compact scheme of high-order on uniformly spaced meshes for a general PPDEs have been suggested in [28]. Mittal and Tripathi [35] developed a numerical method for Burgers-Huxley equation and Burgers-Fisher equation based on collocation of modified cubic B-spline functions.

In the convection-diffusion phenomenon, when convection is significant compared to diffusion, second-order discretization of the convection term gives rise to oscillatory solution values. Such an oscillatory behavior can be resolved by unrealistic small mesh step size or by a high-order accurate method. Many high-order schemes have been developed on uniformly spaced mesh-points, and nearly satisfactory results have been obtained in the past. In the finite-difference approaches, there is a direct connection between truncation error and mesh spacing. The *supra*-convergence of discretization errors indicates that satisfactory numerical solution values can be computed when truncation error exhibit a lower order truncation error [15, 33, 41]. There are two major limitations to finite-difference discretization on uniformly spaced mesh-points. The type of mesh network involves information about solution values and truncation error in the finite-difference discretization depends upon the mesh-step size as well as derivatives of a function. As a result, uniform distribution of local truncation error terms is not possible on uniform meshes. To gain uniform distribution of local truncation error, we need finer meshes in the region for largely deviated derivative and coarse meshes for smooth-function [22, 30]. Such an arrangement of meshes disperses the error almost uniformly over the domain of integration and yields more accurate solution values. Therefore, high-order finite-difference discretization developed on a non-uniformly spaced mesh-point provides stable and accurate solution values.

The present work's core contribution is to develop a high-order accurate, compact scheme for the arbitrary choice of smooth function ψ and describe the effect of variable mesh spacing on the local truncation error. It is shown that the new scheme is fourth-order accurate in the spatial direction and is second-order in the temporal direction for both uniform mesh spacing as well as quasi-variable mesh spacing. The discretization takes one central mesh-point and two adjacent meshes at any time level, producing a compact scheme that is straightforward to implement. In the next section, we discuss quasi-variable meshes and algorithm to determine them. A two-level three-point implicit compact scheme of high-order has been presented in section 3 and their detailed derivations are described in section 4. Application of the new scheme to convection-diffusion equations having singular coefficients has been discussed in section 5. Section 6 presents a detailed stability analysis of the new variable mesh high-order compact scheme for the standard diffusion equation. Numerical illustrations and comparison of quasi-variable meshes compact scheme with uniform meshes compact scheme have been presented in section 7. The paper is finally concluded with remarks, limitations, and future scope.

2. Quasi-variable mesh network

For the discretization purpose, the solution domain $\{(x,t); 0 \le x \le 1, t > 0\}$ is partitioned as $\{(x_n, t_j) : n = 0(1)N + 1, j = 0(1)J\}$, where $0 = x_0 < x_1 < \cdots < x_{N+1} = 1$, $t_j = jk, j = 0(1)J$, and N, J are positive integers and $k = 1/J$ is a fixed time-step. Let $h_n = x_n - x_{n-1}, n = 1(1)N + 1$ be the unequal step-lengths along spatial direction. The subsequent step-length is obtained by $h_{n+1} = (1 + \mu h_n)h_n, n = 1(1)N$. Since, the length of diffusion space is one, thus $\sum_{n=1}^{N+1} h_n = 1$, it is easy to compute the first and subsequent mesh-step size for a given mesh parameter value μ. In particular, when $\mu = 0$, the meshes are evenly spaced and $h = h_n$ for all n. The procedure to generate unequal step-length in spatial direction is presented in the following algorithm:

$$r_1 = 1; r_2 = 1 + \mu; for(n = 3; n \le N + 1; n + +) \ r_n = r_{n-1}(1 + \mu r_{n-1});$$

$$sum = 0; \ for(n = 3; n \le N + 1; n + +) \ sum+ = r_n;$$

$$h_1 = (x_{N+1} - x_0)/sum; \ for(n = 1; n < N; n + +) \ h_{n+1} = h_n(1 + \mu h_n/h_1);$$

$$x_0 = 0; x_{N+1} = 1; \ for(n = 1; n \le N; n + +) \ x_n = x_{n-1} + h_n;$$

Now, let us take a uniform partition of the domain $\mathcal{S} = [0,1] = \{s_n = nh : n = 0(1)N+1\}, h = 1/(N+1)$. Since $h_n > 0 \ \forall n$, therefore, $h_{n+1} = h_n(1 + \mu h_n/h_1) > h_n$ for $\mu > 0$. Therefore, the finite sequence $\{h_n\}_{n=1}^{N+1}$ of mesh-step size is monotonic for $\mu > 0$. The monotonicity of mesh-step sequence permits us to construct a one-one onto mapping

$$\mathcal{F} : \mathcal{S} \longrightarrow \Omega \text{ such that } \mathcal{F}(s_n) = x_n, n = 0(1)N + 1 \tag{2.1}$$

and the Jacobian $J(s) = d\mathcal{F}(s)/ds$ is bounded below and above by some positive constants $(0 < r \le J(s) \le R < \infty, \ \forall s \in \mathcal{S})$. Thus,

$$J(s) > 0 \Rightarrow \frac{d\mathcal{F}(s)}{ds} > 0 \Rightarrow \frac{\mathcal{F}(s_{n+1}) - \mathcal{F}(s_n)}{s_{n+1} - s_n} > 0 \Rightarrow \frac{x_{n+1} - x_n}{(n+1)h - nh} > 0. \tag{2.2}$$

This implies, $h_{n+1} > 0$ for all integer values of n. Also,

$$J(s) \le R \Rightarrow \frac{d\mathcal{F}(s)}{ds} \le R \Rightarrow \frac{x_{n+1} - x_n}{(n+1)h - nh} \le R. \tag{2.3}$$

That is, $0 < h_{n+1} \le Rh \ \forall \ n$. Consequently, we find that $\max_n |h_{n+1}| \le Rh$ and

$$\| \boldsymbol{h} \|_\infty \le Rh = \frac{R}{N + 1} \le \frac{R}{N}, \text{ where } \boldsymbol{h} = [h_1, h_2, \cdots, h_n] \text{ is step-length}$$

vector. Therefore,

$$\| \boldsymbol{h} \|_\infty = O(h) = O\left(\frac{1}{N}\right) \text{ and } \| \boldsymbol{h} \|_\infty \to 0 \text{ when } N \to \infty \text{ or } h \to 0.$$

Such a quasi-variable mesh spacing permits three-points second-order accurate discretization to the second-order partial derivatives $W^{xx} = \partial^2 W/\partial x^2$. Private communication between Samarskii and Saul'yev on variable meshes can be found in the literature [1, 44]. One can notice a discussion of this type of mesh network in the circumstances of electrochemical stimulation, wind-driven ocean circulation model, and convection-dominated phenomenon in [12, 16, 31]. The high-order compact scheme on the quasi-variable mesh provides a more precise solution value than those derived on a uniform mesh network. The new scheme uses the mesh-step relation $h_{n+1} = h_n(1 + \mu h_n)$, and it offers a second-order accuracy to the second-order partial derivative. Another variable mesh spacing, such as $h_{n+1} = \mu h_n$, provides only first-order accuracy to the second-order partial derivative, if $\mu \ne 1$. Consequently, the consideration of next step-size $h_{n+1} = h_n(1 + \mu h_n)$, offers a fourth-order accuracy to the nonlinear parabolic PDEs.

3. Two-level implicit compact scheme

Let $W_{n,i} = W(x_n, t_j)$ and $w_{n,j}$ represents the exact and approximate solution values of (1.7)-(1.9) at the mesh-point (x_n, t_j). We shall denote

$$W_{n,j}^x = \left(\frac{\partial W}{\partial x}\right)_{(x_n,t_j)}, W_{n,j}^{xx} = \left(\frac{\partial^2 W}{\partial x^2}\right)_{(x_n,t_j)}, W_{n,j}^t = \left(\frac{\partial W}{\partial t}\right)_{(x_n,t_j)},$$

and take the following approximations into consideration.

$$\tilde{t}_j = \zeta t_{j+1} + (1-\zeta)t_j, \tag{3.1}$$

$$\widetilde{W}_{n+\tau,j} = \zeta W_{n+\tau,j+1} + (1-\zeta)W_{n+\tau,j}, \tau = 0, \pm 1, \tag{3.2}$$

$$\widetilde{W}_{n+\tau,j}^t = [W_{n+\tau,j+1} - W_{n+\tau,j}]/k, \tau = 0, \pm 1, \tag{3.3}$$

$$\begin{bmatrix} \widetilde{W}_{n,j}^x \\ \widetilde{W}_{n+1,j}^x \\ \widetilde{W}_{n-1,j}^x \end{bmatrix} = \mathcal{M} \begin{bmatrix} \widetilde{W}_{n,j} \\ \widetilde{W}_{n+1,j} \\ \widetilde{W}_{n-1,j} \end{bmatrix}, \tag{3.4}$$

$$\mathcal{M} = \begin{bmatrix} \dfrac{\mu}{1+\mu h_n} & \dfrac{1}{(1+\mu h_n)(2+\mu h_n)h_n} & -\dfrac{1+\mu h_n}{(2+\mu h_n)h_n} \\ -\dfrac{2+\mu h_n}{(1+\mu h_n)h_n} & \dfrac{3+2\mu h_n}{(1+\mu h_n)(2+\mu h_n)h_n} & \dfrac{1+\mu h_n}{(2+\mu h_n)h_n} \\ \dfrac{2+\mu h_n}{(1+\mu h_n)h_n} & -\dfrac{1}{(1+\mu h_n)(2+\mu h_n)h_n} & -\dfrac{3+2\mu h_n}{(2+\mu h_n)h_n} \end{bmatrix},$$

$$\tilde{\psi}_{n\pm1,j} = \psi(x_{n\pm1}, \tilde{t}_j, \widetilde{W}_{n\pm1,j}, \widetilde{W}_{n\pm1,j}^x, \widetilde{W}_{n\pm1,j}^t), \tag{3.5}$$

$$\widetilde{\widetilde{W}}_{n,j}^x = \widetilde{W}_{n,j}^x - \vartheta h_n(\tilde{\psi}_{n+1,j} - \tilde{\psi}_{n-1,j}), \tag{3.6}$$

$$\tilde{\tilde{\psi}}_{n,j} = \psi(x_n, \tilde{t}_j, \widetilde{W}_{n,j}, \widetilde{\widetilde{W}}_{n,j}^x, \widetilde{W}_{n,j}^t). \tag{3.7}$$

Using finite Taylor's expansion, one can make a high-order approximation for the one-space dimensional quasi-linear parabolic partial differential equation (1.7). It is given by

$$\epsilon \mathcal{S}_x \widetilde{W}_{n,j} = h_n^2[\beta_1 \tilde{\psi}_{n+1,j} + \beta_0 \tilde{\tilde{\psi}}_{n,j} + \beta_2 \tilde{\psi}_{n-1,j}] + LTE, \tag{3.8}$$

where $n = 1(1)N, j = 0, 1, 2, \cdots$ and

$$LTE = O(h_n^2 k^2 + h_n^4 k + h_n^6), \tag{3.9}$$

is the local truncation error (LTE) of the scheme,

$$\beta_0 = \frac{2\mu^2 h_n^2 + 5\mu h_n + 5}{6(1+\mu h_n)}, \beta_1 = \frac{3\mu h_n + 1}{6(1+\mu h_n)(2+\mu h_n)}, \beta_2 = \frac{(1+\mu h_n)(1-2\mu h_n)}{6(2+\mu h_n)}, \tag{3.10}$$

and

$$\mathcal{S}_x \widetilde{W}_{n,j} = \frac{2}{(2+\mu h_n)(1+\mu h_n)}\widetilde{W}_{n+1,j} - \frac{2}{1+\mu h_n}\widetilde{W}_{n,j} + \frac{2}{2+\mu h_n}\widetilde{W}_{n-1,j}. \tag{3.11}$$

The new quasi-variable mesh discretization method (3.8) yields a scheme of order four in space and two in time. If λ_n denotes the mesh-ratio parameter, then by choice of time step-size $k \approx \lambda_n h_n^2$, it yields the local truncation error $LTE \approx O(h_n^6)$. Consequently, the order of the scheme (3.8) is $h_n^{-2}LTE \approx O(h_n^4)$ for μ to be zero or non-zero. In other words, we have obtained fourth-order accurate difference formula on a uniform mesh-network and quasi-variable mesh-network as well. We observe

consistency of the difference scheme (3.8) as $LTE \to 0$, when $\max_n h_n \to 0$. For the algorithmic implementations, we omit the truncation error and combine it with the initial and boundary data

$$W_{n,0} = \phi(x_n), W_{0,j} = F_1(t_j), W_{N+1,j} = F_2(t_j), n = 0(1)N + 1, j = 0(1)J. \tag{3.12}$$

The compact character of the two-level scheme results in tri-diagonal Jacobian matrix system. It is solved by a standard iterative method to obtain $W_{(n,0)}, n = 1(1)N + 1, j = 0(1)J$ at internal mesh-points. The difference scheme for the generalized Burgers-Huxley equation (1.1) and Burgers-Fisher equation (1.5) can be obtained by substituting $\psi = W^t + \alpha W^\rho W^x + \beta W(W^\rho - 1)(W^\rho - \sigma)$ and $\psi = W^t + \alpha W^\rho W^x + \beta W(W^\rho - 1)$ respectively in the equation (1.7).

4. Derivation of the compact scheme

To derive the high-order compact scheme, we need to construct operators that approximate first-, and second-order derivatives along the spatial direction in such a manner that they use the minimum number of stencils. By the help of linear combinations of solution values $W_{n,j}$ and $W_{n\pm1,j}$ evaluated at the central mesh-point (x_n, t_j) and their neighbouring mesh-points $(x_{n\pm1}, t_j)$ respectively, one obtains

$$\mathcal{F}_x W_{n,j} = \frac{1}{(1 + \mu h_n)(2 + \mu h_n)} W_{n+1,j} + \frac{\mu h_n}{1 + \mu h_n} W_{n,j} - \frac{1 + \mu h_n}{2 + \mu h_n} W_{n-1,j}, \tag{4.1}$$

$$\mathcal{S}_x W_{n,j} = \frac{2}{(1 + \mu h_n)(2 + \mu h_n)} W_{n+1,j} - \frac{2}{1 + \mu h_n} W_{n,j} + \frac{2}{2 + \mu h_n} W_{n-1,j}, \tag{4.2}$$

$$\mathcal{F}_t W_{n,j} = W_{n,j+1} - W_{n,j}. \tag{4.3}$$

Then, the application of series expansion yields

$$\mathcal{F}_x W_{n,j} = h_n W_{n,j}^x + O(h_n^3), \tag{4.4}$$

$$\mathcal{S}_x W_{n,j} = h_n^2 W_{n,j}^{xx} + O(h_n^4), \tag{4.5}$$

$$\mathcal{F}_t W_{n,j} = k W_{n,j}^t + O(k^2), \tag{4.6}$$

In particular, the operator $\mathcal{S}_x$ reduces to the well-known second-central difference operator $\delta^2 W_{n,j} = W_{n+1,j} - 2W_{n,j} + W_{n-1,j}$ commonly applied to discretize the diffusion-term when a uniform mesh step size is taken into consideration. Similarly, $\mathcal{F}_x$ represents the twice multiple of the composite of averaging and central-difference operators. Such operators application gives rise to *supra* convergent scheme and is useful for solving fully nonlinear parabolic equations in one-dimension, with a lower order or accuracy [15, 41].

Now, let us consider the time-dependent second-order equation

$$\epsilon W^{xx} = \psi(x, t), 0 < x < 1, t > 0. \tag{4.7}$$

At the mesh-point (x_n, t_j), equation (4.7) is represented by

$$\epsilon W_{n,j}^{xx} = \psi(x_n, t_j) \equiv \psi_{n,j}. \tag{4.8}$$

Now, let us consider the linear combination

$$\chi \equiv \chi(x_n, t_j) = h_n^2 [p\psi_{n,j} + qh_n\psi_{n,j}^x + rh_n^2\psi_{n,j}^{xx}], \tag{4.9}$$

By the use of (4.2) and (4.8) in the equation (4.9), we obtain

$$\chi = \epsilon p \mathcal{S}_x W_{n,j} - \frac{h_n^3}{3}\epsilon(p\mu h_n - 3q)W_{n,j}^{xxx} - \frac{h_n^4}{12}\epsilon(p + p\mu h_n - 12r)W_{n,j}^{xxxx} + O(h_n^6). \tag{4.10}$$

The coefficient of h_n^3 and h_n^4 in (4.10) vanishes for the following choices

$$q = \frac{p}{3}\mu h_n, r = \frac{p}{12}(1 + \mu h_n), \tag{4.11}$$

and for all values of p. But the choice $p = 0$ collapses the linear combination (4.9). Thus, any non-zero finite value of p serves our purpose and therefore, for simplicity we take $p = 1$. As a result, the linear combination (4.9) has sixth-order of local truncation error and is given by

$$\chi = \epsilon \mathcal{S}_x W_{n,j} + O(h_n^6). \tag{4.12}$$

Now, the following finite-difference replacements

$$\psi_{n,j}^x = \frac{1}{h_n}\mathcal{F}_x \psi_{n,j} \text{ and } \psi_{n,j}^{xx} = \frac{1}{h_n^2}\mathcal{S}_x \psi_{n,j}, \tag{4.13}$$

in the expression (4.9) and equating it with (4.12), we obtain a Numerovs type scheme on quasi-variable meshes for the time-dependent second-order equation (4.7) in the following manner

$$\epsilon \mathcal{S}_x W_{n,j} = h_n^2[\beta_1 \psi_{n+1,j} + \beta_0 \psi_{n,j} + \beta_2 \psi_{n-1,j}] + T_n, n = 1(1)N, j = 0, 1, \cdots \tag{4.14}$$

where $T_n = O(h_n^6)$ is the sixth-order local truncation error and values of $\beta_\tau, \tau = 0, 1, 2$ are the same as defined in (3.10).

Now, we extend the scheme (4.14) to the quasi-linear parabolic partial differential equation (1.7) that involves first-order spatial and temporal derivative as a non-linear term. To achieve high-order scheme, we need a finite series expansion of the approximations (3.2)-(3.7) and are obtained as follows:

$$\widetilde{W}_{n,j} = W_{n,j} + \zeta k W_{01} + \zeta k^2 W_{02}/2 + O(k^3), \tag{4.15}$$

$$\widetilde{W}_{n+1,j} = W_{n+1,j} + \zeta k W_{01} + \zeta k h_n W_{11} + \widehat{T}_n, \tag{4.16}$$

$$\widetilde{W}_{n-1,j} = W_{n-1,j} + \zeta k W_{01} - \zeta k h_n W_{11} + \widehat{T}_n, \tag{4.17}$$

$$\widetilde{W}_{n,j}^t = W_{n,j}^t + k W_{02}/2 + O(k^2), \tag{4.18}$$

$$\widetilde{W}_{n+1,j}^t = W_{n+1,j}^t + k W_{02}/2 + k h_n W_{12}/2 + \widehat{T}_n, \tag{4.19}$$

$$\widetilde{W}_{n-1,j}^t = W_{n-1,j}^t + k W_{02}/2 - k h_n W_{12}/2 + \widehat{T}_n, \tag{4.20}$$

$$\widetilde{W}_{n,j}^x = W_{n,j}^x + \zeta k W_{11} + h_n^2(1 + \mu h_n)W_{30}/6 + \widehat{T}_n, \tag{4.21}$$

$$\widetilde{W}_{n+1,j}^x = W_{n+1,j}^x + \zeta k(W_{11} + h_n W_{21}) - h_n^2(3\mu h_n + 2)W_{30}/6 - h_n^3 W_{40}/12 + \widehat{T}_n, \tag{4.22}$$

$$\widetilde{W}_{n-1,j}^x = W_{n-1,j}^x + \zeta k(W_{11} - h_n W_{21}) - h_n^2(\mu h_n + 2)W_{30}/6 + h_n^3 W_{40}/12 + \widehat{T}_n, \tag{4.23}$$

where $\widehat{T}_n = O(h_n^4 + h_n^2 k + k^2)$ and $W_{l,m} = \left.\frac{\partial^{l+m}W}{\partial x^l \partial t^m}\right|_{(x_n,t_j)}, l, m = 0(1)4.$

The functional approximations (3.5) in its expanded form are given by

$$\tilde{\psi}_{n+1,j} = \psi_{n+1,j} + \zeta k[(B_n^j + h_n \dot{B}_n^j)W_{01} + \{C_n^j + h_n(B_n^j + \dot{C}_n^j)\}W_{11}] + k(D_n^j + h_n \dot{D}_n^j)W_{02}/2$$
$$- h_n^2[(2 + 3\mu h_n)C_n^j + 2h_n \dot{C}_n^j]W_{30}/6 + \zeta k h_n C_n^j W_{21} + k h_n D_n^j W_{12}/2$$
$$+ \zeta k(A_n^j + h_n \dot{A}_n^j) - h_n^3 C_n^j W_{40}/12 + O(h_n^4 + h_n^2 k + k^2), \tag{4.24}$$

$$\tilde{\psi}_{n-1,j} = \psi_{n-1,j} + \zeta k[(B_n^j - h_n \dot{B}_n^j)W_{01} + \{C_n^j - h_n(B_n^j + \dot{C}_n^j)\}W_{11}] + k(D_n^j - h_n \dot{D}_n^j)W_{02}/2$$
$$- h_n^2[(2 + \mu h_n)C_n^j - 2h_n \dot{C}_n^j]W_{30}/6 - \zeta k h_n C_n^j W_{21} - k h_n D_n^j W_{12}/2$$
$$+ \zeta k(A_n^j - h_n \dot{A}_n^j) + h_n^3 C_n^j W_{40}/12 + O(h_n^4 + h_n^2 k + k^2), \tag{4.25}$$

The additional approximation of the first-order derivative (3.6) is therefore given by

$$\widetilde{\widetilde{W}}_{n,j}^x = W_{n,j}^x + \zeta k W_{11} - \frac{h_n^6}{6}[6\vartheta\epsilon(2 + \mu h_n) - 1 - \mu h_n]W_{30} + O(h_n^4 + h_n^2 k + k^2), \tag{4.26}$$

The new approximation (3.7) at the central mesh-point is therefore expanded as

$$\tilde{\tilde{\psi}}_{n,j}^x = \psi_{n,j} + \zeta k[A_n^j + B_n^j W_{01} + C_n^j W_{11}] + k D_n^j W_{02}/2$$
$$- \frac{h_n^2}{6}C_n^j[6\vartheta\epsilon(2 + \mu h_n) - 1 - \mu h_n]W_{30} + O(h_n^4 + h_n^2 k + k^2), \tag{4.27}$$

At the mesh-point (x_n, t_j), the partial derivative of the quasi-linear equation (1.7) is given by

$$\epsilon W_{21} = A_n^j + B_n^j W_{01} + C_n^j W_{11} + D_n^j W_{02}, \tag{4.28}$$

where

$$A_n^j = \left.\frac{\partial\psi}{\partial t}\right|_{(x_n,t_j)}, B_n^j = \left.\frac{\partial\psi}{\partial W}\right|_{(x_n,t_j)}, C_n^j = \left.\frac{\partial\psi}{\partial W^x}\right|_{(x_n,t_j)}, D_n^j = \left.\frac{\partial\psi}{\partial W^t}\right|_{(x_n,t_j)},$$

and

$$\dot{A}_n^j = \left.\frac{\partial^2\psi}{\partial x \partial t}\right|_{(x_n,t_j)}, \dot{B}_n^j = \left.\frac{\partial^2\psi}{\partial x \partial W}\right|_{(x_n,t_j)}, \dot{C}_n^j = \left.\frac{\partial^2\psi}{\partial x \partial W^x}\right|_{(x_n,t_j)}, \dot{D}_n^j = \left.\frac{\partial^2\psi}{\partial x \partial W^t}\right|_{(x_n,t_j)}.$$

Substituting (4.24)-(4.28) in (3.8), one obtains

$$-\epsilon \mathcal{S}_x \widetilde{W}_{n,j} + h_n^2[\beta_1 \tilde{\psi}_{n+1,j} + \beta_0 \tilde{\tilde{\psi}}_{n,j} + \beta_2 \tilde{\psi}_{n-1,j}]$$
$$= h_n^4[1 + \mu h_n - 10\epsilon\vartheta(2 + \mu h_n)]C_n^j W_{30}/12 + k h_n^2(1 - 2\zeta)D_n^j W_{02}$$
$$+ O(k h_n^4 + k^2 h_n^2 + h_n^6). \tag{4.29}$$

To obtain $O(k h_n^4 + k^2 h_n^2 + h_n^6)$-accurate local truncation error of the scheme (4.29) in the compact operator form, the coefficients of W_{30} and W_{02} in equation (4.29) must vanish. This is possible for the following values of the free parameters,

$$\vartheta = \frac{1 + \mu h_n}{10\epsilon(2 + \mu h_n)}, \zeta = \frac{1}{2}. \tag{4.30}$$

Consequently, the local truncation error to the scheme (3.8) is given by

$$LTE = O(k h_n^4 + k^2 h_n^2 + h_n^6). \tag{4.31}$$

When the mesh-step size in the temporal direction is directly proportional to the square of mesh-step size in the spatial direction, that is $k \propto h_n^2$, or equivalently regarding the mesh ratio parameter λ_n, the substitution $k = \lambda_n h_n^2$ in the scheme (3.8) results in $LTE \approx O(h_n^6)$. The sixth-order magnitude of the local truncation error remains unchanged for zero or non-zero values of μ. That is to say, the compact scheme (3.8) is fourth-order accurate for both evenly spaced mesh-points and variably spaced mesh-points.

5. Difference scheme for convection-diffusion parabolic problems

The mathematical model involving a combination of a diffusive and convective phenomenon is important in fluid dynamics [14]. Determination of temperature in compressible flows, the concentration of a pollutant in fluids and momentum relation of the Navier-Stokes equation are some of the prominent areas of applications to the following form of equations

$$W^t = \epsilon W^{xx} + a(x)W + b(x)W^x = g(x,t), 0 < x < 1, t > 0, \tag{5.1}$$

along with the initial and boundary data (1.8)-(1.9). We will determine the concentration $W(x,t)$ for a small value of viscosity coefficient $\epsilon, (0 < \epsilon << 1)$ and it is given that the functions a and b are smooth in the interior domain. In general, this initial-boundary value problem possesses a unique solution whose smoothness depends on the initial data as well as the magnitude of the viscosity coefficient. The precise analysis of equation (5.1) is essential due to the presence of multiple characters of solution values and occurrence of exponential and / or boundary layer. Application of discretization scheme (3.8) to the linear equation (5.1) yields a linear system of difference equation as

$$\Upsilon_0^+ W_{n,j+1} + \Upsilon_1^+ W_{n+1,j+1} + \Upsilon_2^+ W_{n-1,j+1} = \Upsilon_0^- W_{n,j} + \Upsilon_1^- W_{n+1,j} + \Upsilon_2^- W_{n-1,j} + R_{n,j}, \tag{5.2}$$

with the discrete initial and boundary data

$$W_{n,0} = \phi(x_n), W_{0,j} = F_1(t_j), W_{N+1,j} = F_2(t_j), n = 0(1)N + 1, j = 0(1)J. \tag{5.3}$$

where

$$\Upsilon_0^\pm = \epsilon/(1 + \mu h_n) - \beta_2 h_n^2[(1 + \mu h_n)(ka_n \mp 2) + k\mu b_n]/[2k(1 + \mu h_n)]$$
$$+ h_n^2(\mu h_n + 2)[b_{n+1}(\vartheta h_n b_n \beta_2 + \beta_1) + \beta_2 b_{n-1}(\vartheta h_n b_n - 1)]/[2h_{n+1}], \tag{5.4}$$

$$\Upsilon_1^\pm = -\epsilon/[(\mu h_n + 2)(1 + \mu h_n)] + h_n^2(\vartheta h_n b_n \beta_2 + \beta_1)(\pm 2 - ka_{n+1})/(2k) - h_n^2[\beta_2 b_n$$
$$+ (3 + 2\mu h_n)(\vartheta h_n b_n \beta_2 + \beta_1)b_{n+1} + \beta_2 b_{n-1}(\vartheta h_n b_n - 1)]/[2(\mu h_n + 2)h_{n+1}], \tag{5.5}$$

$$\Upsilon_2^\pm = -\epsilon/(\mu h_n + 2) + \beta_2 h_n^2(ka_{n-1} \mp 2)(\vartheta h_n b_n - 1)/(2k) + [h_n(1 + \mu h_n)(b_n \beta_2 - b_{n+1}(\vartheta h_n b_n \beta_2 + \beta_1))$$
$$- h_n \beta_2(3 + \mu h_n)(\vartheta h_n b_n - 1)b_{n-1}]/[2(\mu h_n + 2)], \tag{5.6}$$

$$R_{n,j} = h_n^2[\beta_2 g_{n,j} + (\beta_1 + \vartheta \beta_2 h_n b_n)g_{n+1,j} + \beta_2(1 - \vartheta b_n h_n)g_{n-1,j}], \tag{5.7}$$

and $a_n = a(x_n), b_n = b(x_n), g_{n,j} = g(x_n, t_j)$.

The general scheme (5.2) has the order of consistency $O(kh_n^6 + h_n^6)$ for any value of $\mu \in [0, 1)$, provided W is continuously differentiable with respect to x and t. Apart from the viscosity effect, the presence of singular points in reaction coefficient $a(x)$ and /or in convection coefficients $b(x)$ inside and on the domain $[0, 1]$, needs special attention. Suppose $a(x) = e^{1/x}$, then $a_{n-1} = e^{1/x_{n-1}}$ and at $n = 1, a_0 = e^{1/x_0}$. Since $x_0 = 0$, the value of a_0 is unbounded, and it halts computing procedure. Such a situation can be resolved by the application of Taylors series as

$$a_{n-1} = e^{1/x_n}\left(1 + \frac{h_n}{x_n^2} + \frac{h_n^2}{2x_n^4}(1 + 2x_n) + \frac{h_n^3}{6x_n^6}(1 + 6x_n + 6x_n^2)\right) + O(h_n^4), \tag{5.8}$$

and on neglecting higher order terms, it is easy to evaluate a_{n-1} at $n = 1$. A similar treatment for the function $b(x)$ can be performed, if it possesses singular behaviour inside and on the domain. The substitution (5.8) and similar expansions for a_{n+1} and $b_{n\pm1}$ in the difference equation (5.2) yields a scheme that is free from the terms $a_{n\pm1}, b_{n\pm1}$ and thus easily computed in the vicinity of singularity.

6. Stability analysis

A compact scheme's stability concerns how truncation error or rounding error behaves as the numerical procedure continues. The von Neumann analysis uses Fourier series representation of error to track its behaviour when a partial differential equation is discretized by finite differences [45]. We consider the standard diffusion equation

$$\epsilon W^{xx} = W^t, 0 < x < 1, t > 0, \tag{6.1}$$

The application of quasi-variable meshes high-order compact scheme (3.8) to (6.1) gives the fully discrete scheme

$$\gamma_0^+ W_{n,j+1} + \gamma_1^+ W_{n+1,j+1} + \gamma_2^+ W_{n-1,j+1} = \gamma_0^- W_{n,j} + \gamma_1^- W_{n+1,j} + \gamma_2^- W_{n-1,j}, n = 1(1)N, j = 0, 1, \cdots \tag{6.2}$$

where

$$\gamma_0^{\pm} = [2\mu^2 h_n^2 + 5\mu h_n + 5 \pm 6\epsilon\lambda_n]/[6\lambda_n(1 + \mu h_n)],$$
$$\gamma_2^{\pm} = -[2\mu^2 h_n^2 + \mu h_n - 1 \pm 6\epsilon\lambda_n]/[6\lambda_n(2 + \mu h_n)],$$
$$\gamma_1^{\pm} = [3\mu h_n + 1 \mp 6\epsilon\lambda_n]/[6\lambda_n(1 + \mu h_n)(2 + \mu h_n)],$$
$$\gamma_0^{\pm} + \gamma_1^{\pm} + \gamma_2^{\pm} = 1/\lambda_n,$$

and $\lambda_n \approx k/h_n^2$ is the mesh-ratio parameter.

Let $E_{n,j} = W_{n,j} - w_{n,j} = \xi^j e^{i\theta x_n}$ be the point-wise error at the mesh-point (x_n, t_j), where ξ is a complex number, and θ is an arbitrary real number. The norm $|\xi|$ represents the time-dependent amplitude of the initial error. The point-wise error satisfies the relation

$$\gamma_0^+ E_{n,j+1} + \gamma_1^+ E_{n+1,j+1} + \gamma_2^+ E_{n-1,j+1} = \gamma_0^- E_{n,j} + \gamma_1^- E_{n+1,j} + \gamma_2^- E_{n-1,j}, n = 1(1)N, j = 0, 1, \cdots \tag{6.3}$$

Since, $x_{n+1} = x_n + h_{n+1}$ and $x_{n-1} = x_n - h_n$, therefore, the expression $E_{n,j} = \xi^j e^{i\theta x_n}$ enables us to substitute

$$E_{n+1,j+1} = E_{n,j+1} e^{i\theta h_{n+1}}, \ E_{n+1,j} = E_{n,j} e^{i\theta h_{n+1}},$$
$$E_{n-1,j+1} = E_{n,j+1} e^{-i\theta h_n}, \ E_{n-1,j} = E_{n,j} e^{-i\theta h_n},$$

in the equation (6.3). As a consequence, the amplification factor takes the form

$$\xi = \frac{1 + \lambda_n \psi(\theta)}{1 - \lambda_n \psi(\theta)}, \ \psi(\theta) = \frac{A + iB}{C + iD}, \tag{6.4}$$

where

$$A = 12\epsilon[2 + \mu h_n - (1 + \mu h_n)\cos(\theta h_n) - \cos(\theta h_{n+1})],$$
$$B = 12\epsilon[(1 + \mu h_n)\sin(\theta h_n) - \sin(\theta h_{n+1})],$$
$$C = 2(2\mu h_n - 1)(\mu h_n + 1)^2 \cos(\theta h_n) - 2(3\mu h_n + 1)\cos(\theta h_{n+1}) - 2(\mu h_n + 2)(2\mu^2 h_n^2 + 5\mu h_n + 5),$$
$$D = 2(\mu h_n + 1)^2(1 - 2\mu h_n)\sin(\theta h_n) - 2(1 + 3\mu h_n)\sin(\theta h_{n+1}).$$

For the stability of two-level implicit scheme (6.3), we need to prove $|\xi|^2 \leq 1$. That is,

$$\frac{\lambda_n^2(A^2 + B^2) + 2\lambda_n(AC + BD) + C^2 + D^2}{\lambda_n^2(A^2 + B^2) - 2\lambda_n(AC + BD) + C^2 + D^2} \leq 1. \tag{6.5}$$

Equivalently, for stability, it suffices to prove $AC + BD \leq 0$. Upon trigonometric simplification, we obtain

$$
\begin{aligned}
AC + BD = & - 96\epsilon\lambda_n(\mu h_n + 2)(\mu h_n + 1)(2\mu^2 h_n^2 + 3\mu h_n + 2)\sin^2(\theta h_n/2) \\
& - 96\epsilon\lambda_n(\mu h_n + 2)(\mu^2 h_n^2 + \mu h_n + 2)\sin^2(\theta h_{n+1}/2) \\
& - 96\epsilon\lambda_n(\mu h_n + 1)(1 + \mu h_n - \mu^2 h_n^2)\sin^2(\theta(h_n + h_{n+1})/2).
\end{aligned} \tag{6.6}
$$

It is easy to observe that $AC + BD \leq 0$, because $1 + \mu h_n - \mu^2 h_n^2 = 1 + \mu h_n(1 - \mu h_n) > 0$, since $0 < h_n < 1, 0 \leq \mu < 1$ and ϵ, λ_n are positive real numbers [34]. As a result, we conclude that the scheme (6.2) is unconditionally stable.

7. Computational experiments

To illustrate the proposed scheme, we have computed accuracies in approximate solution values $w_{n,j}$ and exact solution values $W_{n,j}$ using the metrics maximum absolute (MA), root-mean-squared (RMS) errors and numerical convergence order Θ_∞ and Θ_2. They are defined in the following manner

$$
\| \epsilon \|_\infty^{(N)} = \max_{n=1(1)N, j=1(1)J} | W_{n,j} - w_{n,j} |, \quad \Theta_\infty = \log_2\left(\frac{\| \epsilon \|_\infty^{(N)}}{\| \epsilon \|_\infty^{(2N+1)}}\right),
$$

$$
\| \epsilon \|_2^{(N)} = \sqrt{\frac{1}{NJ}\sum_{n=1}^{N}\sum_{j=1}^{J} | W_{n,j} - w_{n,j} |^2}, \quad \Theta_2 = \log_2\left(\frac{\| \epsilon \|_2^{(N)}}{\| \epsilon \|_2^{(2N+1)}}\right).
$$

The norm values are determined for both the mesh spacing; quasi-variable meshes ($\mu \neq 0$) and uniform mesh step sizes ($\mu = 0$). As a test procedure, the initial and boundary values are determined from the analytical solution values. Thomas algorithm (tri-diagonal solver) and Newton's iterative method solve the linear and nonlinear difference equations respectively. For Newton's iterative method, the absolute error tolerance value is taken as 10^{-12} with an initial guess as zero vectors [25]. In all the computations, we have chosen mesh ratio parameter $\lambda_n = 1.6$ and the number of temporal steps $J = (N + 1)^2/\lambda_n$, so that $k \approx \lambda_n h_n^2$ and hence, it is practical to verify the fourth-order of convergence to new numerical scheme. Maple's *CodeGeneration* has been applied to generate difference equations, and numerical computations are performed in C on Mac OS.

Example 7.1. We consider one-dimensional GBHE (1.1)-(1.3) along with analytic solution (1.4) and compare the numerical solutions for the various values of parameters. For $\epsilon = 1, \alpha = 10, \beta = 100, \rho = 2$ and $\sigma = 0.4, 0.6, 0.8$, experiments with uniform meshes compact scheme (3.8) for $\mu = 0$ yields unstable solution while the quasi-variable meshes high-order compact scheme (3.8) for $\mu \neq 0$ gives rise to accurate solution in conformity with order and accuracies of the new scheme as shown in Table 1 at the time level $t = 1$. For all the values of σ, the value of mesh parameter μ is kept fixed, to analyze the effect of σ on the order and accuracies of solutions.

Case 1: *Huxley equation*: By taking $\alpha = 0, \beta = \epsilon = 1$, in the equation (1.1)-(1.3) and its analytical solution (1.4), we present measurements of accuracies in solution values for a fixed value of $\sigma = 0.001$ and various values of ρ in Table 2.

Case 2: *Burgers-Huxley equation*: By taking $\alpha = -1, \beta = \rho = \epsilon = 1$ in the equation (1.1)-(1.3) and its analytical solution (1.4), we have reported maximum absolute errors, root-mean-square errors in the solution for a fixed value of $\sigma = 10$ in Table 3. A comparative result about solution accuracy is obtained in Table 4 using $\alpha = \beta = \epsilon = \rho = 1$ and $\sigma = 10^{-3}$ at the mesh parameter value $\mu = 10^{-3}$ and

TABLE 1. MA and RMS errors and computational order in example 7.1

$N+1$	μ	$\|\|\epsilon\|\|_\infty^{(N)}$	$\|\|\epsilon\|\|_2^{(N)}$	Θ_∞	Θ_2
$\sigma = 0.8$					
8	0.2820	$6.81e-03$	$4.89e-03$	$--$	$--$
16	0.0980	$4.08e-04$	$2.77e-04$	4.1	4.1
32	0.0391	$2.80e-05$	$1.17e-05$	4.0	4.6
64	0.0176	$1.71e-06$	$3.90e-07$	4.0	4.9
$\sigma = 0.6$					
8	0.2820	$4.26e-03$	$3.09e-03$	$--$	$--$
16	0.0980	$2.88e-04$	$1.94e-04$	3.9	4.0
32	0.0391	$1.85e-05$	$7.73e-06$	4.0	4.7
64	0.0176	$1.12e-06$	$2.54e-07$	4.0	4.9
$\sigma = 0.4$					
8	0.2820	$2.04e-03$	$1.51e-03$	$--$	$--$
16	0.0980	$1.77e-04$	$1.20e-04$	3.5	3.7
32	0.0391	$1.02e-05$	$4.26e-06$	4.1	4.8
64	0.0176	$6.08e-07$	$1.38e-07$	4.1	4.8

TABLE 2. MA and RMS errors and computational order in example 7.1

$N+1$	μ	$\|\|\epsilon\|\|_\infty^{(N)}$	$\|\|\epsilon\|\|_2^{(N)}$	Θ_∞	Θ_2
$\rho = 2$					
8	0.1800	$2.14e-06$	$1.65e-06$	$--$	$--$
16	0.0100	$1.30e-07$	$9.82e-08$	4.0	4.1
32	0.0003	$7.51e-09$	$5.57e-09$	4.1	4.1
64	$1.0e-05$	$3.20e-10$	$2.40e-10$	4.6	4.5
$\rho = 4$					
8	0.1800	$1.11e-05$	$8.55e-06$	$--$	$--$
16	0.0100	$6.75e-07$	$5.09e-07$	4.0	4.1
32	0.0003	$3.91e-08$	$2.90e-08$	4.1	4.1
64	$1.0e-05$	$2.53e-09$	$1.87e-09$	3.9	4.0
$\sigma = 5$					
8	0.1800	$1.48e-05$	$1.14e-05$	$--$	$--$
16	0.0100	$9.01e-07$	$6.80e-07$	4.0	4.1
32	0.0003	$5.22e-08$	$3.87e-08$	4.1	4.1
64	$1.0e-05$	$3.38e-09$	$2.49e-09$	3.9	4.0

TABLE 3. MA and RMS errors and computational order in example 7.1

$N+1$	μ	$\|\|\epsilon\|\|_\infty^{(N)}$	$\|\|\epsilon\|\|_2^{(N)}$	Θ_∞	Θ_2
8	0.2400	$1.52e-02$	$7.51e-03$	$--$	$--$
16	0.0880	$8.95e-04$	$2.46e-04$	4.1	4.9
32	0.0378	$5.54e-05$	$1.06e-05$	4.0	4.5
64	0.0174	$3.54e-06$	$5.07e-07$	4.0	4.4

TABLE 4. MA errors with $\mu = 10^{-3}, \alpha = \beta = \epsilon = \rho = 1$ and $\sigma = 10^{-3}$ in Example 7.1

Our x	t	Proposed Scheme	x	Ref. [29]	Ref. [38]	Ref. [4]
	1.00	5.0671e-11		1.1296e-08	1.1288e-08	3.7481e-08
0.0995	0.10	3.3956e-11	0.1	1.6864e-08	1.6858e-08	3.7481e-07
	0.05	2.3229e-11		7.7273e-09	7.7266e-09	1.8740e-08
	1.00	1.4116e-10		2.8830e-08	2.8825e-08	3.7437e-08
0.4990	0.10	8.6922e-11	0.5	4.6849e-08	4.6844e-08	3.7210e-07
	0.05	5.2333e-11		1.7353e-08	1.7348e-08	1.8739e-08
	1.00	1.4116e-10		1.1298e-08	1.1291e-08	3.7481e-08
0.9000	0.10	8.6922e-11	0.9	1.6866e-08	1.6860e-08	3.6842e-07
	0.05	5.2333e-11		7.7278e-09	7.7273e-09	1.8725e-08

TABLE 5. MA and RMS errors and computational order in example 7.1

$N+1$	μ	$\|\epsilon\|_\infty^{(N)}$	$\|\epsilon\|_2^{(N)}$	Θ_∞	Θ_2
8	0.2400	$6.80e-03$	$3.38e-03$	$--$	$--$
16	0.0880	$3.73e-04$	$1.03e-04$	4.2	4.9
32	0.0378	$2.02e-05$	$3.87e-06$	4.2	4.7
64	0.0174	$1.26e-06$	$1.81e-07$	4.0	4.4

TABLE 6. MA and RMS errors and computational order in example 7.1

$N+1$	μ	$\|\epsilon\|_\infty^{(N)}$	$\|\epsilon\|_2^{(N)}$	Θ_∞	Θ_2
$\sigma = 10$					
8	0.2400	$1.38e-02$	$6.88e-03$	$--$	$--$
16	0.0880	$7.46e-04$	$2.06e-04$	4.2	5.1
32	0.0378	$4.05e-05$	$7.74e-06$	4.2	4.7
64	0.0174	$2.52e-06$	$3.62e-07$	4.0	4.4
$\sigma = 20$					
8	0.2400	$1.11e-01$	$6.07e-02$	$--$	$--$
16	0.0880	$3.10e-03$	$8.56e-04$	5.2	6.1
32	0.0378	$1.62e-04$	$3.10e-05$	4.3	4.8
64	0.0174	$1.01e-05$	$1.45e-06$	4.0	4.4
$\sigma = 40$					
8	0.2400	$1.14e-00$	$6.53e-01$	$--$	$--$
16	0.0880	$3.52e-02$	$9.78e-03$	5.0	6.1
32	0.0378	$6.93e-04$	$1.32e-04$	5.7	6.1
64	0.0174	$4.04e-05$	$5.80e-06$	4.1	4.5

$J = 10^3, N = 9$.

Case 3: *Zeldovich equation*:By taking $\alpha = 0$, $\rho = \epsilon = 1$ in the equation (1.1)-(1.3) and its analytical solution (1.4), the numerical estimates are presented in Table 5 for $\beta = 4$ and $\sigma = 5$.

TABLE 7. MA and RMS errors and computational order in example 7.1

$N+1$	μ	$\|\epsilon\|_\infty^{(N)}$	$\|\epsilon\|_2^{(N)}$	Θ_∞	Θ_2
4	0.97000	$1.30e-01$	$7.68e-02$	$--$	$--$
8	0.29400	$9.17e-03$	$3.60e-03$	3.8	4.4
16	0.09610	$8.52e-04$	$2.22e-04$	3.4	4.0
32	0.03917	$6.85e-05$	$1.28e-05$	3.6	4.1

TABLE 8. MA and RMS errors and computational order in example 7.1

$N+1$	μ	$\|\epsilon\|_\infty^{(N)}$	$\|\epsilon\|_2^{(N)}$	Θ_∞	Θ_2
4	0	$2.72e-08$	$1.58e-08$	$--$	$--$
8	0	$5.05e-09$	$1.98e-09$	2.4	3.0
16	0	$3.23e-10$	$1.23e-10$	4.0	4.0
32	0	$1.76e-11$	$5.52e-12$	4.0	4.5
4	0.0640	$1.45e-08$	$1.11e-08$	$--$	$--$
8	0.5980	$9.15e-10$	$3.46e-10$	4.0	5.0
16	0.1247	$5.72e-11$	$1.73e-11$	4.0	4.3
32	0.0457	$3.50e-12$	$7.78e-13$	4.0	4.5

TABLE 9. MA and RMS errors and computational order in example 7.2

$N+1$	μ	$\|\epsilon\|_\infty^{(N)}$	$\|\epsilon\|_2^{(N)}$	Θ_∞	Θ_2
8	0	$3.64e-02$	$1.87e-02$	$--$	$--$
16	0	$1.32e-02$	$5.11e-03$	1.5	1.9
32	0	$1.50e-03$	$5.58e-04$	3.1	3.2
64	0	$1.14e-04$	$4.15e-05$	3.7	3.8
8	0.2200	$8.92e-02$	$3.37e-02$	$--$	$--$
16	0.0210	$8.70e-03$	$3.61e-03$	3.4	3.2
32	0.0008	$7.72e-04$	$2.35e-04$	3.5	3.9
64	$2.0e-05$	$5.63e-05$	$1.58e-05$	3.8	3.9

TABLE 10. MA and RMS errors and computational order in example 7.2

$N+1$	μ	$\|\epsilon\|_\infty^{(N)}$	$\|\epsilon\|_2^{(N)}$	Θ_∞	Θ_2
4	0.700	$3.93e-02$	$3.29e-02$	$--$	$--$
8	0.245	$8.07e-04$	$4.51e-04$	5.6	6.2
16	0.090	$6.91e-05$	$2.29e-05$	3.5	4.3
32	0.038	$3.69e-06$	$7.01e-07$	4.2	4.9

Case 4: *Fitzhug-Nagumo equation*: By taking $\alpha = 0, \beta = \rho = \epsilon = 1$, in the equation (1.1)-(1.3) and its analytical solution (1.4), we present measurements of accuracies for various values of σ in Table 6. For $\sigma \leq 5$, uniform meshes high-order compact scheme produces an oscillation-free solution.

TABLE 11. MA and RMS errors and computational order in example 7.2

$N+1$	μ	$\|\epsilon\|_\infty^{(N)}$	$\|\epsilon\|_2^{(N)}$	Θ_∞	Θ_2
$\beta = 10^3$					
4	0	$1.45e-02$	$8.43e-03$	$--$	$--$
8	0	$2.93e-02$	$1.11e-02$	-1.0	-0.4
16	0	$2.38e-03$	$6.14e-03$	0.3	0.8
4	0.600	$8.12e-02$	$4.84e-02$	$--$	$--$
8	0.147	$9.92e-03$	$3.77e-03$	3.0	3.7
16	0.044	$8.97e-04$	$3.22e-04$	3.5	3.5
$\beta = 10^4$					
4	0	$1.92e-03$	$1.11e-03$	$--$	$--$
8	0	$6.59e-02$	$2.50e-03$	-1.8	-1.2
16	0	$1.51e-02$	$3.91e-03$	-1.2	-0.6
4	0.9700	$9.91e-02$	$5.85e-02$	$--$	$--$
8	0.0300	$8.10e-03$	$3.08e-03$	3.6	4.2
16	0.0788	$6.22e-04$	$2.03e-04$	3.7	4.0

TABLE 12. MA and RMS errors and computational order in example 7.3

$N+1$	μ	$\|\epsilon\|_\infty^{(N)}$	$\|\epsilon\|_2^{(N)}$	Θ_∞	Θ_2
$\alpha = 1/2$					
4	$1.0e-02$	$5.01e-02$	$3.60e-02$	$--$	$--$
8	$3.0e-04$	$3.86e-03$	$2.73e-03$	3.7	3.7
16	$1.0e-05$	$2.88e-04$	$1.94e-04$	3.7	3.8
32	$3.0e-07$	$1.79e-05$	$1.19e-05$	4.0	4.0
$\alpha = -1/2$					
4	$1.0e-02$	$1.16e-01$	$8.73e-02$	$--$	$--$
8	$3.0e-04$	$1.06e-02$	$8.15e-03$	3.5	3.4
16	$1.0e-05$	$7.98e-04$	$6.21e-04$	3.7	3.7
32	$3.0e-07$	$5.03e-05$	$3.92e-05$	4.0	4.0
$\alpha = 0$					
4	0	$7.80e-04$	$5.66e-04$	$--$	$--$
8	0	$7.84e-05$	$5.08e-05$	3.3	3.5
16	0	$6.90e-06$	$4.25e-06$	3.5	3.6
32	0	$5.93e-05$	$3.37e-07$	3.5	3.7

Case 5: *Burgers equation*: For $\alpha = \rho = 1$, $\beta = 0$ and $0 < \epsilon << 1$, the equation (1.1)-(1.3) possesses a solitary wave solution [7] as

$$W(x,t) = \frac{1}{2} - \frac{1}{2}\tanh\left(\frac{1}{4\epsilon}(x - \frac{t}{2})\right), \tag{7.1}$$

and another theoretical solution to the Burger's equation is

$$W(x,t) = \frac{2\epsilon\pi\sin(\pi x)e^{-\epsilon\pi^2 t}}{2 + \cos(\pi x)e^{-\epsilon\pi^2 t}}. \tag{7.2}$$

TABLE 13. MA and RMS errors and computational order in example 7.4

$N+1$	μ	$\|\epsilon\|_\infty^{(N)}$	$\|\epsilon\|_2^{(N)}$	Θ_∞	Θ_2
$\epsilon = 10^{-1}$					
4	0	$6.24e-02$	$5.24e-02$	$--$	$--$
8	0	$1.68e-02$	$1.31e-02$	2.0	2.0
16	0	$4.35e-03$	$3.23e-03$	2.0	2.0
32	0	$1.09e-04$	$7.97e-04$	2.0	2.0
4	0.9000	$7.13e-04$	$5.34e-01$	$--$	$--$
8	0.0800	$5.97e-05$	$4.75e-02$	3.6	3.5
16	0.0070	$3.86e-06$	$3.07e-03$	4.0	4.0
32	0.0004	$3.01e-07$	$1.97e-04$	3.7	4.0
$\epsilon = 10^{-2}$					
4	0	$7.87e-02$	$6.80e-02$	$--$	$--$
8	0	$2.32e-02$	$1.84e-02$	1.8	1.9
16	0	$5.93e-03$	$4.53e-03$	2.0	2.0
32	0	$1.49e-03$	$1.12e-03$	2.0	2.0
4	0.9000	$6.62e-01$	$4.79e-01$	$--$	$--$
8	0.0800	$5.88e-02$	$4.42e-02$	3.5	3.4
16	0.0030	$4.44e-03$	$3.05e-03$	3.7	3.7
32	0.0023	$3.57e-04$	$2.56e-04$	4.0	4.0

TABLE 14. MA and RMS errors and computational order in example 7.5

$N+1$	μ	$\|\epsilon\|_\infty^{(N)}$	$\|\epsilon\|_2^{(N)}$	Θ_∞	Θ_2
$\epsilon = 10^{-2}$					
16	0	$7.53e-04$	$4.50e-04$	$--$	$--$
32	0	$9.17e-04$	$4.97e-04$	-0.2	-0.1
64	0	$3.31e-04$	$1.75e-04$	1.5	1.5
16	0.0650	$5.69e-04$	$3.81e-04$	$--$	$--$
32	0.0180	$3.82e-05$	$1.91e-05$	3.9	4.3
64	0.0019	$1.60e-06$	$8.52e-07$	4.6	4.5
$\epsilon = 10^{-3}$					
16	0	$6.64e-02$	$5.34e-02$	$--$	$--$
32	0	$3.18e-02$	$2.10e-02$	1.1	1.3
64	0	$6.10e-03$	$3.41e-03$	2.4	2.6
16	0.0100	$5.47e-02$	$4.45e-02$	$--$	$--$
32	0.0320	$4.06e-03$	$2.76e-03$	3.7	4.0
64	0.0167	$3.60e-04$	$2.08e-04$	3.5	3.7

The numerical experiments with solitary wave solution (7.1) fails to capture the behaviour of error estimates at $\epsilon = 2^{-8}$ in case of uniform meshes high-order method ($\mu = 0$). By employing quasi-variable high-order compact scheme, it is possible to measure the accuracies of solution values regarding maximum absolute error and order of convergence (Table 7). The solution curve for $\epsilon = 2^{-2}, 2^{-4}, 2^{-6}$ and 2^{-8} are shown in Figure 1(a)-1(d), respectively and it is evident that the smoothness of solution deteriorates for decreasing values of ϵ. On the other hand, there is little effect on the measure of accuracies of

TABLE 15. MA and RMS errors and computational order in example 7.5

$N+1$	μ	$\|\epsilon\|_\infty^{(N)}$	$\|\epsilon\|_2^{(N)}$	Θ_∞	Θ_2
$\epsilon = 10^{-3}$					
16	0	$5.66e-02$	$2.27e-02$	$--$	$--$
32	0	$8.67e-03$	$2.54e-03$	2.7	3.2
64	0	$6.52e-04$	$1.92e-04$	3.7	3.7
16	0.1185	$3.27e-04$	$8.45e-05$	$--$	$--$
32	0.0432	$1.66e-05$	$2.97e-06$	4.3	4.8
64	0.0185	$8.47e-07$	$1.07e-07$	4.3	4.8
$\epsilon = 10^{-4}$					
16	0	$5.69e-04$	$3.81e-04$	$--$	$--$
32	0	$3.82e-05$	$1.91e-05$	3.9	4.3
64	0	$1.60e-06$	$8.52e-07$	4.6	4.5
16	0.1185	$9.91e-04$	$2.56e-04$	$--$	$--$
32	0.0432	$5.12e-05$	$9.20e-06$	4.3	4.8
64	0.0185	$2.62e-96$	$3.30e-07$	4.3	4.8

TABLE 16. MA and RMS errors and computational order in example 7.5

$N+1$	μ	$\|\epsilon\|_\infty^{(N)}$	$\|\epsilon\|_2^{(N)}$	Θ_∞	Θ_2
$\epsilon = 10^{-2}$					
16	0	$2.83e-03$	$2.04e-03$	$--$	$--$
32	0	$3.50e-04$	$2.34e-04$	3.0	3.1
64	0	$2.58e-05$	$1.75e-05$	3.8	3.7
128	0	$2.03e-06$	$1.54e-06$	3.7	3.5
16	0.11840	$3.33e-05$	$8.60e-06$	$--$	$--$
32	0.04320	$1.58e-06$	$2.84e-07$	4.4	4.9
64	0.01850	$8.08e-08$	$1.02e-08$	4.3	4.8
128	0.00854	$6.27e-09$	$5.57e-10$	3.7	4.2
$\epsilon = 10^{-3}$					
16	0	$3.20e-03$	$2.34e-03$	$--$	$--$
32	0	$7.85e-04$	$5.63e-04$	2.0	2.1
64	0	$1.53e-04$	$1.06e-04$	2.4	2.4
128	0	$1.47e-05$	$9.37e-06$	3.4	3.5
16	0.1184	$3.22e-05$	$8.36e-06$	$--$	$--$
32	0.0432	$1.59e-06$	$2.86e-07$	4.3	4.9
64	0.0185	$8.15e-08$	$1.03e-08$	4.3	4.8
128	0.00854	$6.33e-09$	$5.62e-10$	3.7	4.2

solution values by using the highly analytic theoretical solution (7.2). For $\epsilon = 10^{-2}, 10^{-3}$ the solution is smooth, and high-order uniform meshes compact scheme yields uniformly accurate solution values as reflected from the computational order of convergence. Therefore, quasi-variable mesh-points are not needed for such solutions. However, the proposed high-order quasi-variable meshes compact scheme gives superior results as compared to uniform meshes compact scheme and results obtained in [43]. The numerical accuracies evaluated at $\epsilon = 10^{-4}$ are shown in Table 8.
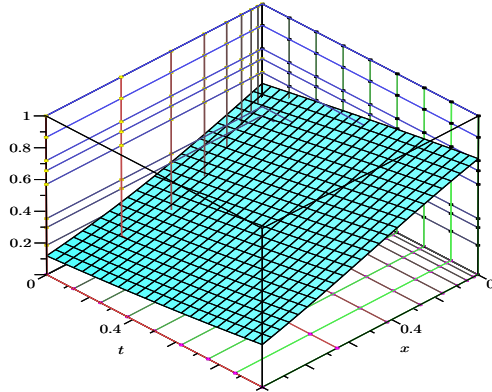
Fig. 1(a) Solution plot in example 7.1 at $\varepsilon = 1/4$
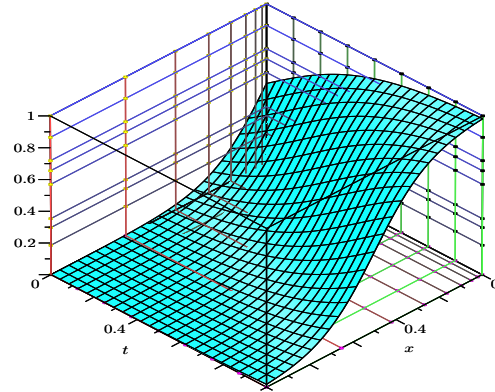
Fig. 1(b) Solution plot in example 7.1 at $\varepsilon = 1/16$
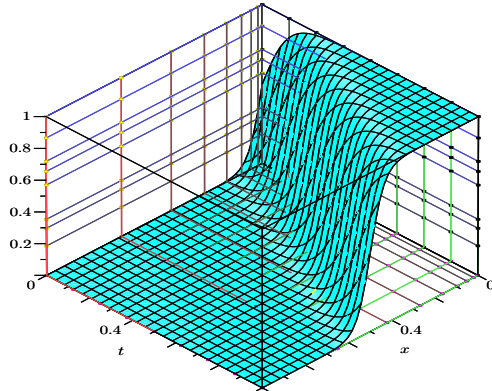
Fig. 1(c) Solution plot in example 7.1 at $\varepsilon = 1/64$
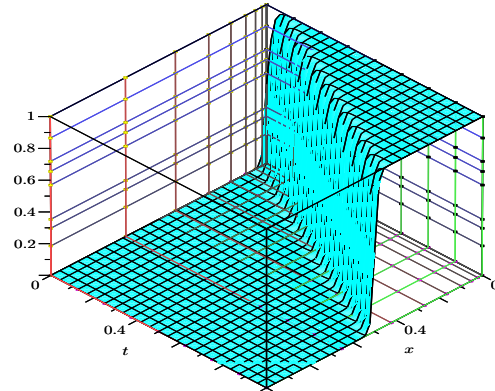
Fig. 1(d) Solution plot in example 7.1 at $\varepsilon = 1/256$

FIGURE 1. Solution plots for examples 7.1 at different values of ϵ.

Example 7.2 We consider one-dimensional Generalized Burger's-Fisher equation (1.5) along with the following associated initial and boundary values

$$W(x,0) = \left[\frac{1}{2} - \frac{1}{2}\tanh\left(\frac{\alpha\rho}{2\epsilon(1+\rho)}x\right)\right]^{1/\rho},$$

$$W(0,t) = \left[\frac{1}{2} - \frac{1}{2}\tanh\left(\frac{-\alpha\rho(\alpha^2 + \epsilon\beta(1+\rho)^2)t}{2\epsilon\alpha(1+\rho)^2}t\right)\right]^{1/\rho},$$

$$W(1,t) = \left[\frac{1}{2} - \frac{1}{2}\tanh\left(\frac{\alpha\rho}{2\epsilon(1+\rho)}\left(1 - \frac{\alpha^2 + \epsilon\beta(1+\rho)^2}{\alpha(1+\rho)}t\right)\right)\right]^{1/\rho}.$$

and it possess analytical solution as

$$W(x,t) = \left[\frac{1}{2} - \frac{1}{2}\tanh\left(\frac{\alpha\rho}{2\epsilon(1+\rho)}\left(x - \frac{\alpha^2 + \epsilon\beta(1+\rho)^2}{\alpha(1+\rho)}t\right)\right)\right]^{1/\rho}, \alpha \neq 0 \qquad (7.3)$$

At the time level $t = 1$, we will demonstrate accuracies in the solution values for $\alpha = \beta = \rho = 1$ and $\epsilon = 2^{-6}$ in Table 9. By using $\mu \neq 0$, the order and accuracies conform with our proposed method, and

exhibit superiority over the corresponding uniform meshes high-order compact scheme.

Case 1: *Fisher's equation*: By taking $\alpha = 0, \rho = \epsilon = 1$ in the equation (1.5), the solution (7.3) does not work due to zero divisor. Therefore, we take the analytical solution as

$$W(x,t) = \left[1 + \exp\left(\sqrt{\frac{\beta}{6}}x - \frac{5\beta}{6}t\right)\right]^{-2}. \tag{7.4}$$

The numerical experiments show the smooth behaviour of solution values for small values of β, while the large value of β exhibits the oscillatory behaviour of a solution with the uniform meshes high-order scheme [36]. It is possible to achieve a stable solution by using quasi-variable meshes scheme for a large value of $\beta = 100$ in Table 10.

Case 2: *Rayleigh-Benard convection equation*: By taking $\alpha = 0$, $\rho = 2$ and $\epsilon = 1$ in the equation (1.5), we consider the analytical solution as

$$W(x,t) = \frac{e^{\sqrt{\frac{\beta}{2}}x} - e^{-\sqrt{\frac{\beta}{2}}x}}{e^{\sqrt{\frac{\beta}{2}}x} + e^{-\sqrt{\frac{\beta}{2}}x} + e^{-\frac{3\beta t}{2}}}. \tag{7.5}$$

In this case, we have conducted experiments for various values of β. When $\beta < 1$, (say $\beta = 1/10$) , the computed solution values preserve order, as well as accuracy and the same, can be verified from the graphical illustration of the solution curve. When $\beta >> 1$, (say $\beta = 10^3$), the numerical solution values have oscillation in case of uniform meshes high-order compact scheme, and this happens due to loss of smoothness. By considering quasi-variable mesh high-order compact scheme, it is possible to generate order preserving solution values as shown in Table 11.

Example 7.3. We consider the dimensionless diffusion boundary layer equation

$$W^{xx} = W^t + \frac{2\alpha - 1}{x}W^x, \quad 0 < x < 1, t > 0. \tag{7.6}$$

For $\alpha = 0$ and $\alpha = -1/2$, it is a heat equation with axial symmetry and central symmetry respectively, if the spatial variable x is replaced with radial variable r [3]. It is a pure diffusion equation for $\alpha = 1/2$. For $\alpha = 0$, we have achieved stable solution values when uniform meshes compact scheme ($\mu = 0$) is employed, and the effect of quasi-variable meshes is not significant. For $\alpha = \pm 1/2$, the uniform meshes high-order compact scheme ($\mu = 0$) exhibit oscillatory solutions, and therefore, it is necessary to employ quasi-variable meshes compact scheme (3.8) with ($\mu \neq 0$). Note that the scheme's direct application (3.8) to the singular equation (7.6) is not possible. This is because, the evaluation of advection coefficient $\frac{2\alpha-1}{x}$ at the mesh point (x_{n-1}, t_j) is $\frac{2\alpha-1}{x_{n-1}}$ and at $n = 1$, it leads to zero divisibility. The singular behaviour can be resolved by substututing $1/x_{n-1} = \sum_{l=0}^{5} h_n^l x_n^{-(1+l)} + O(h_n^6)$ in the scheme. The resulting difference equation is free from all the singular terms and can be easily evaluated after neglecting higher-order terms. Numerical simulations using the analytic solution

$$W(x,t) = 1 + 16(2-\alpha)(1-\alpha)t^2 + 8(2-\alpha)tx^2 + x^4 \tag{7.7}$$

were performed and the accuracies measured regarding maximum absolute errors and root-mean-squared errors at the time level $t = 1$ are reported in Table 12 along with their computational order of convergence.

Example 7.4. *(Ilkovič's Equation)* Consider the mathematical model that appears in the field of polarography. It describes the heat transfer to the surface of a growing drop and flows out of the thin

capillary into an incompressible fluid solution. The mass of the flow of fluid moving on the capillary is assumed constant, and the the diffusion layer thickness is much less than the radius of the drop. The Ilkovič's equation describes such a model

$$\epsilon W^{xx} = W^t - \frac{x}{t} W^x, \quad 0 < x < 1, t > 0. \tag{7.8}$$

This equation governs the depolarizer's diffusion to the surface of the dropping mercury electrode, where $W(x,t)$ is the concentration of the depolarizer at distance x from electrode surface at time t and ϵ is the diffusion coefficient of the depolarizer. The solution depends on the diffusion coefficient, and when $\epsilon = 0.1$ or for more smaller values, the numerical accuracy of solution values using high-order uniform meshes compact scheme ($\mu = 0$) yields non-satisfactory numerical order. However, a slight change in the mesh-step sizes results in an accurate solution and agrees with the new-scheme's theoretical order. Numerical simulations with uniform meshes and quasi-variable meshes high-order compact scheme has been reported in Table 13 at the time level $t = 1$, using analytical solution $W(x,t) = 1 + \exp(xt + \epsilon t^3/3)$ and accordingly chosen initial and boundary values [3].

Example 7.5. *(Boundary layer problem)* Consider the parabolic problem that possesses singularly perturbed behaviour

$$\epsilon W^{xx} = W^t + cW^x - aW + g(x,t), \quad 0 < x < 1, t > 0. \tag{7.9}$$

We compute the maximum absolute errors and root-mean-squared errors in numerical and following analytic solutions:

$$W(x,t) = e^{-t - \frac{x}{\sqrt{\epsilon}}}, W(x,t) = \cos(\pi t) \left[1 + (x-1)e^{\frac{x}{\sqrt{\epsilon}}} - xe^{\frac{x-1}{\sqrt{\epsilon}}} \right], W(x,t) = e^{-\epsilon t} \sin(\pi x).$$

These solutions exhibit different character as the value of parameters ϵ changes. The first solution [9] exhibit one-sided multiple natures of solution values at $a = c = 1$ (Table 14), the second solution displays both sided multiple behaviour at $a = -0.1, c = 0.1$ (Table 15), while the third solution at $a = 0, c = 10$ has minimal effect of perturbation parameters (Table 16). The solution curve for the second solution is obtained with $\epsilon = 10^{-1}, 10^{-2}, 10^{-3}$ and 10^{-4} are shown in Figure 2(a)-2(d) respectively. The sharpness at both the side increases with decreasing values of ϵ. The accuracy in numerical and analytic solutions is computed at a time level $t = 2$ in each case. The initial and boundary values are determined from the analytic solution as a test procedure.The right-side function $g(x,t)$ and initial-boundary values are determined from the analytic solution. In all the circumstances, quasi-variable meshes high-order compact schemes exhibit stable, accurate, and uniformly convergent solution values compared to the constant mesh-step size high-order scheme.

8. Remarks, limitations and future scope

Based on a quasi-variable meshes network, a new compact scheme of accuracy $O(h_n^4)$ in the spatial direction and $O(k^2)$ in temporal direction has been obtained for the numerical computation of quasilinear PPDEs. The proposed scheme utilizes the minimum number of stencils for the discretization purpose. It refers to quasi-variable meshes and uniform meshes high-order methods of the same order of accuracy, similar to a supra-convergent scheme with a lower order of truncation errors. When the temporal step-size is directly proportional to the square of spatial-step size, the proposed scheme behaves like a fourth-order method. Some of the proposed scheme features are: (a) A single two-level three-point compact scheme represents a fourth-order scheme in uniform meshes and quasi-variable meshes. For a particular choice of mesh parameter $\mu = 0$, it is a fourth-order uniform mesh scheme, and for $\mu \neq 0$, it results in a fourth-order quasi-variable mesh scheme. (b) The truncation error depends on mesh spacing and derivative of the variable. Thus, the uniform distribution of discretization error is
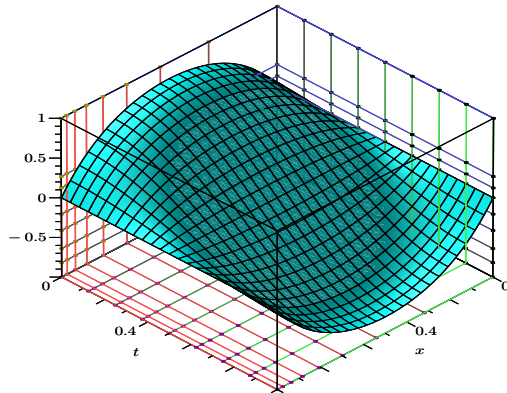
Fig. 2(a) Solution curve in example 7.5 at $\varepsilon = 1/10$
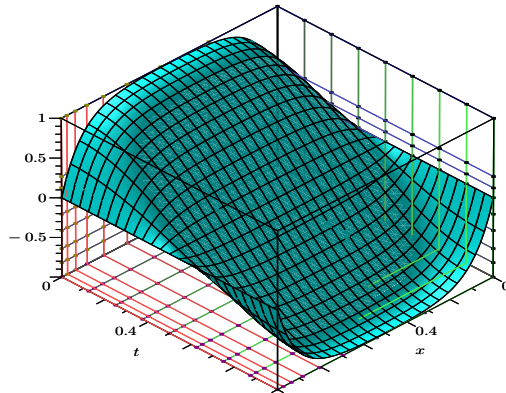
Fig. 2(b) Solution curve in example 7.5 at $\varepsilon = 1/100$
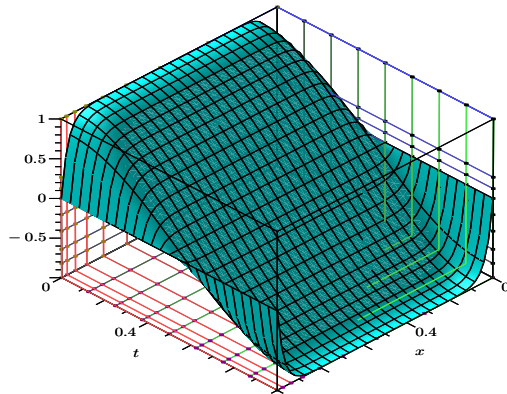
Fig. 2(c) Solution curve in example 7.5 at $\varepsilon = 1/1000$
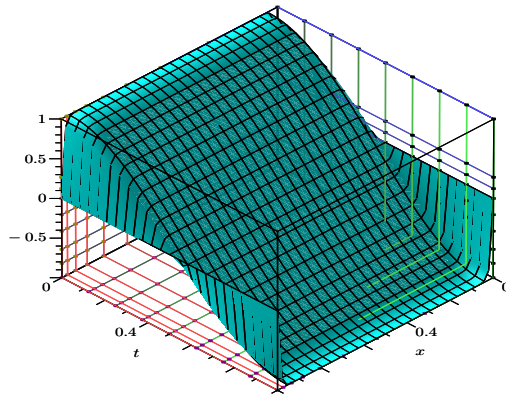
Fig. 2(d) Solution curve in example 7.5 at $\varepsilon = 1/10000$

FIGURE 2. Solution plots for examples 7.2 at different values of ϵ.

possible only through the variable spacing between mesh points. Smaller mesh step-size in the region where derivatives of the function are large and larger spacing in the region where the function is smooth. (c) Quasi-variable mesh high accuracy uses a smaller number of mesh points, iteration numbers, and computing time compared to a uniform mesh high accuracy scheme to achieve the same accuracy order. We have established the von Neumann stability analysis to the standard diffusion equation. Experiments with various values of parameters that appeared in the governing equations have been described in detail and obtained convergent solution values. The error estimates on the new scheme prove superior compared with existing results. Such type of scheme can be extended to higher dimensions PPDEs. Computational results using quasi-variable meshes high-order compact schemes are essential or advantageous compared with the existing high accuracy method.

REFERENCES

[1] A. A. Samarskii, P. P Matus and P. N Vabishchevich, *Difference schemes with operator factors*, Springer, Dordrecht, 2002.

[2] A. C. Newell and J. A. Whitehead, *Finite bandwidth, finite amplitude convection*, J. Fluid Mech. **38**(1969), 279–303.

[3] A. D. Polyanin and V. E. Nazaikinskii, *Handbook of linear partial differential equations for engineers and scientists*, CRC press, Boca Raton, 2015.

[4] A. G. Bratsos, *A fourth order improved numerical scheme for the generalized Burger's-Huxley equation*, Am. J. Comput. Math. **1**(2011), 152-158.

[5] A. Kaushik and M. D. Sharma, *A uniformly convergent numerical method on non-uniform mesh for singularly perturbed unsteady Burgers-Huxley equation*, Appl. Math. Comput. 1**95**(2008), 688-706.

[6] A. M. Wazwaz, *Burgers, Fisher and Related Equations*, In: Partial Differential Equations and solitary waves theory, Nonlinear Phy. Sci., Springer, Berlin, (2009), 665–681.

[7] A. M. Wazwaz, *The tanh method for generalized forms of nonlinear heat conduction and Burgers-Fisher equation*, Appl. Math. Comput. **169**(2005), 321–338.

[8] A. Mohebbi and M. Dehghan, *High-order compact solution of the one-dimensional heat and advection-diffusion equations*, Appl. Math. Model. **34**(2010), 3071–3084.

[9] C. S. Liu and P. Wang, *An analytic adjoint Trefftz method for solving the singular parabolic convection-diffusion equation and initial pollution profile problem*, Int. J. Heat Mass Tran. **101**(2016), 1177–1184.

[10] C. Valls, *Algebraic traveling waves for the generalized Newell-Whitehead-Segel equation*, Nonlinear Anal. Real. **36**(2017), 249–266.

[11] D. Agirseven and T. Ozis, *An analytical study for Fisher type equations by using homotopy perturbation method*, Comput. Math. Appl. **60**(2011), 602–609.

[12] D. Britz, *Digital simulation in electrochemistry*, Springer, Berlin, 2005.

[13] H. Ding and Y. Zhang, *A new difference scheme with high accuracy and absolute stability for solving convection-diffusion equations*, J. Comput. Appl. Math. **230**(2009), 600–606.

[14] H. G. Roos, M. Stynes and L. Tobiska, *Robust numerical methods for singularly perturbed differential equations: convection-diffusion-reaction and flow problems*, Springer Science & Business Media, 24, 2008.

[15] H. O. Kreiss, T. A. Manteuffel, B. Swartz, B. Wendroff and A. B. White, *Supra-convergent schemes on irregular grids*, Math. Comput. **47**(1986), 537–554.

[16] H. Sundqvist and G. Veronis, *A simple finite-difference grid with non-constant intervals*, Tellus A. **22**(1970), 26-31.

[17] I. B. Jacques, *Predictor-corrector methods for parabolic partial differential equations*, Int. J. Numer. Meth. Eng. **19**(1983), 451–465.

[18] I. Celik, *Haar wavelet method for solving generalized Burgers-Huxley equation*, Arab J. Math. Sci. **18**(2012), 25–37.

[19] J. E. Macias-Diaz, *On an exact numerical simulation of solitary-wave solutions of the Burgers-Huxley equation through Cardano's method*, BIT Numer. Math. **54**(2014), 763–776.

[20] J. E. Macias-Diaz, J. Ruiz-Ramirez and J. Villa, *The numerical solution of a generalized Burgers-Huxley equation through a conditionally bounded and symmetry-preserving method*, Comput. Math. Appl. **62**(2011), 3330-3342.

[21] J. Feng, W. Li and Q. Wan, *Using-(G'/G) expansion method to seek the traveling wave solution of Kolmogorov-Petrovskii-Piskunov equation*, Appl. Math. Comput. **217**(2011), 5860–5865.

[22] J. H. Ferziger and M. Peric, *Computational methods for fluid dynamics*, Springer-Verlag Berlin, Heidelberg, 2002.

[23] J. Rashidinia, A. Barati, and M. Nabati, *Application of Sinc-Galerkin method to singularly perturbed parabolic convection-diffusion problems*, Numer. Algor. **66**(2014), 643–662.

[24] J. Rashidinia, M. Ghasemi and R. Jalilian, *A collocation method for the solution of nonlinear one-dimensional parabolic equations*, Mathematical Sciences, **4**(2010), 87-104.

[25] L. A. Hageman and D. M. Young, *Applied Iterative Methods*, Academic Press, New York, 1981.

[26] L. K. Bieniasz, *Improving the accuracy of the spatial discretization in finite-difference electrochemical kinetic simulations by means of the extended Numerov method*, J. Comput. Chem. **25**(2004), 1075–1083.

[27] M. Dehghan, J. M. Heris and A. Saadatmandi, *Application of semi-analytic methods for the Fitzhugh-Nagumo equation, which models the transmission of nerve impulses*, Math. Meth. Appl. Sci. **33**(2010), 1384–1398.

[28] M. K. Jain, R. K. Jain and R. K. Mohanty, *A fourth order difference method for the one-dimensional general quasilinear parabolic partial differential equations*, Numer. Methods Partial Differ. Equ. **6**(1990), 311–319.

[29] M. Sari and G. Gűrarslan, A. Zeytinoğlu, *High-order finite difference schemes for numerical solutions of the generalized Burger's'Huxley equation*, Numer. Methods Partial Differ. Equ. **27**(2011), 1313-1326.

[30] N. Jha and L. K. Bieniasz, *A fifth (six) order accurate, three-point compact finite difference scheme for the numerical solution of sixth order boundary value problems on geometric meshes*, J. Sci. Comput. **64**(2015), 898–913.

[31] N. Jha and N. Kumar, *A fourth-order accurate quasi-variable mesh compact finite-difference scheme for two-space dimensional convection-diffusion problems*, Adv. Differ. Equ. **64**(2017), 1–13.

[32] O. P. Layeni, *New exact solutions for some power law nonlinear diffusion equation*, J. Appl. Math. Comput. **35**(2011), 93–102.

[33] P. A. Forsyth and P. H. Sammon, *Quadratic convergence for cell-centered grids*, Appl. Numer. Math. **4**(1988), 377–394.

[34] R. A. Bernatz, *Fourier series and numerical methods for partial differential equations*, Wiley, New York, 2010.

[35] R. C. Mittal and A. Tripathi., *Numerical solutions of generalized Burgers-Fisher and generalized Burgers-Huxley equations using collocation of cubic B-splines*, Int. J. Comput. Math. **92**(2015), 1053–1077.

[36] R. K. Mohanty and S. Sharma, *High-accuracy quasi-variable mesh method for the system of 1D quasi-linear parabolic partial differential equations based on off-step spline in compression approximations*, Adv. Differ. Equ. **212**(2017), 1–30.

[37] R. K. Mohanty, *An Finite difference method for one-space Burger's equation in polar coordinates*, Numer. Methods Partial Differ. Equ. **12**(1996), 579–583.

[38] R. K. Mohanty, W. Dai and D. Liu, *Operator compact method of accuracy two in time and four in space for the solution of time dependent Burgers-Huxley equation*, Numer. Algor. **70**(2015), 591-605.

[39] R. Mohammadi, *B-Spline collocation algorithm for numerical solution of the generalized Burger's-Huxley equation*, Numer. Methods Partial Differ. Eqns. **29**(2013), 1173-1191.

[40] R. Mohammadi, *Spline solution of the generalized Burgers'-Fisher equation*, Appl. Anal. **91**(2012), 2189-2215.

[41] T. A. Manteuffel and A. B. White, *The numerical solution of second-order boundary value problems on nonuniform meshes*, Math. Comput. **47**(1986), 511–535.

[42] T. Kawahara and M. Tanaka, *Interactions of travelling fronts: an exact solution of a nonlinear diffusion equation*, Phys. Lett. A. **97**(1983), 311–314.

[43] U. Arora, S. Karaa and R. K. Mohanty, *A new stable variable mesh method for 1D non-linear parabolic differential equations*, Appl. Math. Comput. **181**(2013), 1423–1430.

[44] V. K. Saul'yev, *Integration of equations of parabolic type by the method of nets*, Pergamon Press, New York, 1964.

[45] W. Hundsdorfer and J. G. Verwer, *Numerical solution of time-dependent advection-diffusion-reaction equations*, Springer-Verlag, Berlin, Heidelberg, 2013.

[46] Z. F. Tian and P. X. Yu, *A high-order exponential scheme for solving 1D unsteady convection-diffusion equations*, J. Comput. Appl. Math. **235**(2011), 2477-2491.

Corresponding author. Faculty of Mathematics and Computer Science, South Asian University, Akbar Bhawan, Chanakyapuri, New-Delhi, India-110021

E-mail address: `navnitjha@sau.ac.in`

Faculty of Mathematics and Computer Science, South Asian University, Akbar Bhawan, Chanakyapuri, New-Delhi, India-110021

E-mail address: `mdvwg@students.sau.ac.in`